Supercritical CO2 extraction of oil from Moroccan unroasted Argan Kernels: Effects of process parameters to produce cosmetic oil

Adil Mouahid, Magalie Claeys-Bruno, Isabelle Bombarda, Sandrine Amat, Andrea Ciavarella, Emmanuelle Myotte, Jean-Paul Nisteron, Christelle Crampon, Elisabeth Badens

Supercritical CO_2 extraction of oil from Moroccan unroasted Argan Kernels: Effects of process parameters to produce cosmetic oil

Adil Mouahid [a,*], Magalie Claeys-Bruno [b], Isabelle Bombarda [b], Sandrine Amat [b], Andrea Ciavarella [a], Emmanuelle Myotte [a], Jean-Paul Nisteron [a], Christelle Crampon [a], Elisabeth Badens [a]

[a] Aix Marseille Univ, CNRS, Centrale Marseille, M2P2, Marseille, France
[b] Aix Marseille Univ, Avignon Université, CNRS, IRD, IMBE, Marseille, France

ARTICLE INFO

Keywords:
Argania spinosa L.
Supercritical CO_2 extraction
Response surface methodology
Process parameters
Cosmetic oil

ABSTRACT

The effects of process parameters: pressure (200 – 400 bar), temperature (313 – 333 K), and flow rate (0.11 – 0.27 kg/h) on the efficiency of extraction process of Argan oil by supercritical CO_2 were investigated using response surface methodology and mathematical modelling (Sovová's mathematical model). The fastest extraction kinetics corresponding to the optimal operating conditions were obtained at 400 bar, 333 K at a CO_2 flow rate of 0.11 kg corresponding to a residence time of about 8.8 min. A tocopherol rich oil can be obtained at the beginning of the extraction experiment.

1. Introduction

The oil extracted from Argan kernels is a product of high added value used in food, cosmetics, and pharmaceutical industries. Cosmetic, beauty and edible oils are the three different types of oil produced from Argan kernels [1], the processes for producing these oils are shown in Fig. 1. From unroasted kernels, cosmetic and beauty oils are produced while edible oil is produced from roasted kernels. Beauty and edible oils are produced in Morocco while cosmetic oil is mainly produced in Europe. The cosmetic oil used as ingredient for cosmetic products is obtained by organic solvent (cyclohexane, petroleum ether, chloroform, or dichloromethane) extraction. After extraction, a separation step is needed to separate the solvent from the oil. The extraction yield of cosmetic oil is about 45–50%. The beauty oil is used to be applied on the skin or hair; it is obtained by mechanical cold-pressed extraction. Before the bottling, the oil settles naturally for 15 days and then is centrifuged. The extraction yield of beauty oil is about 40 – 45%.

The edible oil is obtained by mechanical cold-pressed extraction with an extraction yield of 40–45% or by traditional millstone extraction with an extraction yield of 25 – 30%. The sediments are separated from the oil by applying the same separation steps than those applied for the beauty oil.

Argan kernels can contain up to 63% of oil [2], the extraction processes reported in Fig. 1 never lead to the highest reachable oil amount. Furthermore, separation steps (settling, solvent evaporation), which can be long and expensive, are necessary to obtain the final oil. It is worth noting that traces of sediments or organic solvents, which are known to be toxic, can be found in the oils.

Supercritical CO_2 (SC-CO_2) extraction is a very good alternative to organic solvent extraction as CO_2 is non-toxic, its solvent power and selectivity towards neutral lipids can be improved by tuning temperature and pressure. Moreover, no separation step is needed since CO_2 is gaseous at ambient conditions of pressure and temperature. Lastly, CO_2 is recycled at industrial scale enabling a green and compact process. To our knowledge, four studies dealing with the SC-CO_2 extraction of argan oil were reported in the literature [2–5]. Taribak et al. [3] have extracted argan oil from 100 to 400 bar at temperatures from 308 to 328 K with a CO_2 flow rate of 1.2 kg/h. The extractions lasted for 3 h, no extraction kinetics were reported. The SC-CO_2 extraction yields varied between a few percent (100 bar at 318 and 328 K) to 48% (400 bar and 318 K). The authors reported that at a set temperature the yield increased with increasing pressure. A retrograde solubility zone was reported for pressures up to 200 bar, while at pressures upper and equal to 300 bar the extraction yield was independent of temperature. No significant differences were observed between the physicochemical parameters of the oils extracted at different conditions of pressure and temperature: the quality of the oil did not vary significantly compared to the oil extracted using press or *n*-hexane extraction. Haloui et al. [4] have performed SC-CO_2 extractions of argan oil from southeast of

* Corresponding author.
E-mail address: adil.mouahid@univ-amu.fr (A. Mouahid).

Nomenclature

a_g	specific surface area of the biomass powder (m^{-1})
a_s	specific area between the regions of intact and broken cells (m^{-1})
C_u	solute content in the untreated solid ($kg_{oil}/kg_{biomass}$)
D_{21}	diffusion coefficient of oil (2) to CO_2 (1) (m^2/s)
d_p	mean particle diameter (m)
e	extraction yield of mathematical model ($kg_{oil}/kg_{insoluble\ biomass}$)
E	amount extracted (kg)
k_f	fluid-phase mass transfer coefficient (s^{-1})
k_s	solid-phase mass transfer coefficient (m/s)
K	partition coefficient
n	number of experimental points
N	solid charge in the extractor (kg)
N_m	charge of insoluble solid (kg)
P	pressure (bar)
q	relative amount of the passed solvent ($kg_{CO2}/kg_{insoluble\ biomass}$)
$q_{60\%}$	CO_2/biomass mass ratio ($kg_{CO2}/kg_{biomass}$) for reaching a yield of 60%
q'	specific flow rate ($kg_{solvent}/kg_{solid}/s$)
$\dot{Q}$	solvent flow rate (kg/s)
r	grinding efficiency or fraction of broken cells
T	temperature (K)
t	extraction time (s)
t_r	SC-CO_2 residence time in the extraction autoclave (min)
t_f	extraction time to achieve the SC-CO_2 extraction (h)
V	CO_2 velocity in empty autoclave (m/s)
x_t	transition concentration ($kg_{oil}/kg_{insoluble\ solid}$)
x_u	concentration in the untreated solid ($kg_{oil}/kg_{insoluble\ biomass}$)
y_s	solute apparent solubility (kg_{oil}/kg_{CO2})

Greek letters

γ	solvent to matrix ratio in the bed ($kg_{solvent}/kg_{insoluble\ solid}$)
ε	bed void fraction

Algeria (Tindouf). Extraction experiments ranged from 100 to 400 bar, temperatures from 308 to 328 K at a CO_2 flow rate of 0.252 kg/h. The extractions lasted for 2 h, no extraction kinetics were reported. At 100 bar, the yield was found to be lower than 7%. A retrograde solubility behaviour was reported at 250 bar. The study reported by Mouahid et al. [2] aimed to deepen the two previous ones by reporting the extraction kinetics at pressure ranges from 200 to 400 bar and temperature ranges from 313 to 333 K. It was shown that it was possible to reach the highest amount of extractible oil (about 63%) whatever the operating conditions, the fastest extraction kinetics were obtained at 400 bar and 333 K with a CO_2 flow rate of 0.14 kg/h and a mean particle size diameter of 750 μm. A lower granulometry (mean particle size diameter of 400 μm) led to the slowest extraction kinetics probably due to channelling. A retrograde solubility behaviour was highlighted when the extraction was performed at pressures lower than 300 bar, a similar tendency was found when SC-CO_2 extraction was performed on other oleaginous (Jatropha and Walnuts) [6–9]. In addition, the extraction curves exhibit solute-matrix interactions which can be described with a good accuracy by type B Sovová's mathematical model [10], at 200 bar the extraction of tocopherols seems to occur at the beginning of the extraction process. Recently, Mechqoq et al. [5] studied the quality of Argan oil extracted by conventional (cold press extraction and Soxhlet extraction with *n*-hexane) and green extraction methods (SC-CO_2 extraction and enzyme assisted extraction). They evaluated the oil quality parameters by determining the acid, peroxide and iodine values and the extinction coefficients at 232 and 270 nm (K_{232} and K_{270}). It was shown that all the extracted oils showed a good oxidation stability according to the official Argan oil norm [11]. The same SC-CO_2 operating conditions as Taribak et al. [3] were applied in their study leading to similar SC-CO_2 extraction yields: 25 up to 50% depending on the operating conditions. No extraction kinetics were reported. The highest oil extraction yield (66%) was obtained after enzymatic extraction for 24 h

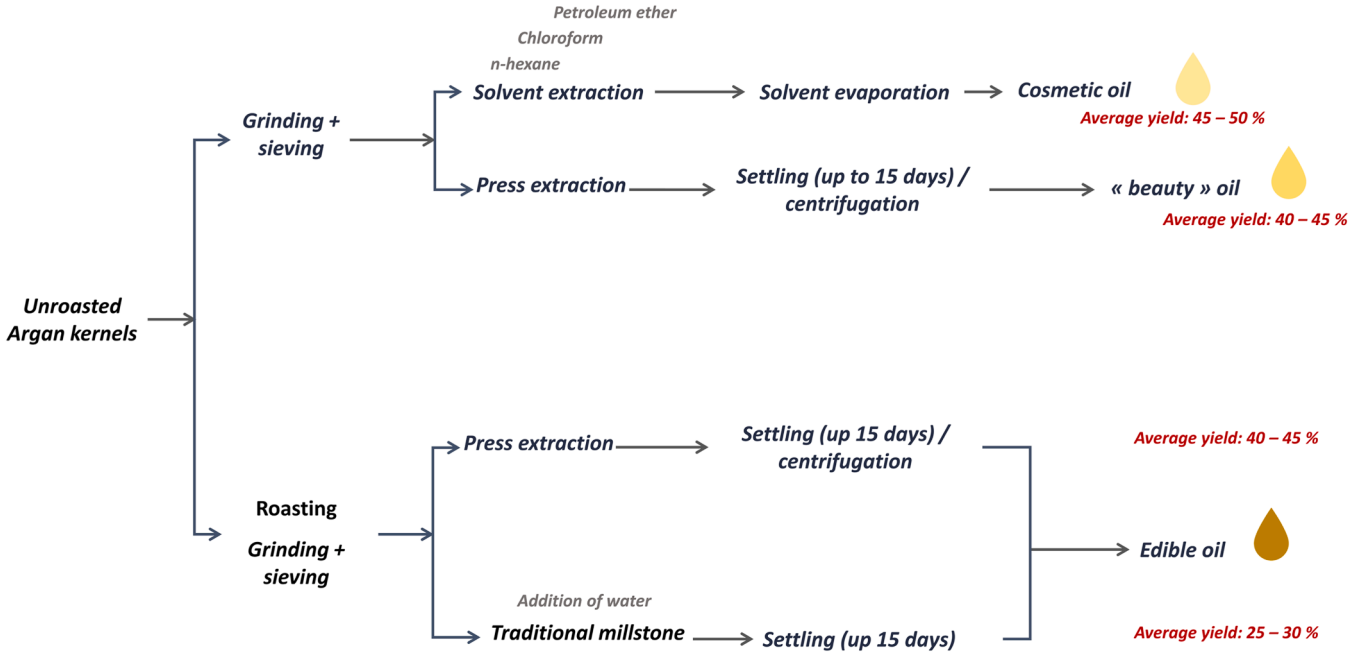

Fig. 1. Different types of Argan oil extraction depending on the application field.

followed by centrifugation and funnel decantation.

This study is the continuation of Mouahid et al. study [2]. It aims to establish the optimal operating conditions for the extraction of unroasted Argan oil by SC-CO_2 for cosmetic applications. To our knowledge these optimal parameters were not established in the literature. Response Surface Methodology (RSM) [12] was applied to study the effects of pressure, temperature, and flow rate on the extraction kinetics, Argan oil apparent solubility in SC-CO_2 and the CO_2/biomass mass ratio corresponding to an extraction yield of 60%. The extraction kinetics reported in the previous study at 0.14 kg/h [2] were considered to evaluate the effects of pressure and temperature by RSM. Additional extraction experiments were performed at pressure range of 300–400 bar, temperature range of 313–333 K and at a CO_2 flow rate range from 0.11 to 0.18 kg/h to evaluate the effects of flow rate and temperature. The fatty acids (FA) composition of the extracts was determined and the effects of the CO_2/biomass mass ratio on the tocopherol composition of extracted Argan oil were also discussed.

2. Materials and methods

2.1. Raw material and chemicals

Argan fruits were collected in September 2019 from southwest Morocco (Essaouira region) and sun dried for few days. The dried nuts were manually shelled to get the kernels. Unroasted argan kernels were grinded and sieved at a mean particle diameters "d_p" of 750 μm. Samples were stored at 277 K prior to SC-CO_2 extraction experiments to avoid degradation of oil. No drying was applied on the kernels. CO_2 was provided by Air Liquide (France) with a purity of 99.7%.

2.2. SC-CO_2 extraction

SC-CO_2 extraction experiments were performed on a laboratory scale extractor supplied by Separex (Champigneulles, France). An extraction autoclave of 20 cm^3 (internal length: 16 cm, internal diameter: 1.2 cm) was used for the study. The detailed configuration of the extractor was given in previous study [2]. For each experiment, the mass introduced in the extraction autoclave lies between 6 and 7 g. Regarding the small charges used for SC-CO_2 extraction experiments, the mass of extracted oil was estimated relative to the mass losses of the sample in the extraction autoclave. The yield was calculated considering Eq. (1).

$$Yield\ (kg/kg) = \frac{mass\ of\ extracted\ oil\ (kg)}{biomass\ introduced\ in\ the\ extractor\ (kg)} \quad (1)$$

The extraction curves were plotted as the variation of the yield as function of the CO_2/biomass mass ratio.

2.3. Gas chromatography analysis

The extracted oils were transesterified to obtain fatty acid methyl esters (FAME) which were analyzed by gas chromatography (Agilent gas chromatograph 7890 A, Agilent Technologies Inc., Santa Clara, California). Hydrogen was used as a carrier gas with a flow of 1 mL/min. The instrument was equipped with a split/split-less injector (split ratio 1:60), a flame ionization detector and a Supelcowax 10 (Merck KGaA, Darmstadt, Germany) silica capillary column coated with polyethylene glycol (L × ID 60 m × 0.25 mm, df 0.25 μm). The following temperature gradient was applied: 210 °C during 20 min, then from 210° to 245°C at 6 °C/min, and 245 °C for 20 min. The data acquisition and processing were performed using Chemstation B.04.03-SPA (87) (Agilent) software.

3. Modelling

3.1. Experimental design

The effects of operating conditions: pressure, temperature and flow rate were investigated using response surface methodology (RSM), all parameters were calculated using Azurad software. As the highest reachable yield was the same for all operating conditions, the apparent solubility of Argan oil in SC-CO_2 (y_s) and the value of CO_2/biomass mass ratio corresponding to an oil extraction yield of 60% ($q_{60\%}$) were selected as responses. In the "results and discussions" part, it will be explained why y_s refer to the apparent solubility and not the solubility.

These parameters are decisive criteria to examine the possibility of applying SC-CO_2 process for the extraction of the overall oil contained in the Argan kernels at industrial scale and drawing up the scale-up calculations. Each response Y was modelled using a second-order polynomial model (Eq. (2)).

$$Y = b_0 + b_iX_i + b_jX_j + b_{ii}X_i^2 + b_{jj}X_j^2 + B_{ij}X_i \cdot X_j \text{ were } X_i \text{ and } X_j \text{ are coded values} \quad (2)$$

The effects of pressure and temperature were investigated considering a classical plan (central composite design) composed of 9 experiments (plan A). Three levels (corresponding to coded values −1, 0, 1) were considered for the pressure (200, 300 and 400 bar), the temperature (313, 323 and 333 K), at a constant flow rate of 0.14 kg/h.

The effect of temperature and flow rate was studied at a constant pressure of 400 bar, considering a plan (central composite design) composed of 9 experiments (plan B). Three levels (corresponding to coded values −1, 0, 1) were considered for the temperature (313, 323 and 333 K), and the flow rate (0.11, 0.14 and 0.18 kg/h). The experiments performed for each plan were reported in Table 1.

3.2. Broken and Intact Cells (BIC) model

The extraction curves were modelled using Type B Sovová's BIC mathematical model [10]. The first part of the extraction curve is composed of two straight lines (Fig. 2) described by Eqs. (3)−(6). The first straight line (Eq. (3)) is controlled by solute solubility in SC-CO_2. The second straight line (Eq. (5)) indicates that the solute concentration in the biomass is considerably reduced, and the equilibrium is controlled by solute-matrix interactions. This implies that the solute concentration in the supercritical phase is much lower than its solubility. The transition between the two straight lines occurs at the transition concentration x_t: the solid-phase concentration became lower than "x_t" and all the solute interacted with the matrix. Hence, the transfer no longer depends on solubility but on the partition coefficient K which represents the constant of proportionality of the linear relationship between solid and fluid-phase concentrations. The transition concentration x_t is equal to the matrix capacity for interaction with the solute.

Solute-matrix interactions can be related to the desorption of the

Table 1
Experiments performed for studying the effect of pressure, temperature, and flow rate.

	Plan A: Effect of pressure and temperature Q = 0.14 kg/h		Plan B: Effect of temperature and flow rate P = 400 bar	
Experiments	**X_i = P (bar)**	**X_j = T (K)**	**X_i = T (K)**	**X_j = Q (kg/h)**
1	200	313	313	0.11
2	200	323	333	0.11
3	200	333	313	0.18
4	300	313	333	0.18
5	300	323	313	0.14
6	300	333	333	0.14
7	400	313	323	0.11
8	400	323	323	0.18
9	400	333	323	0.14

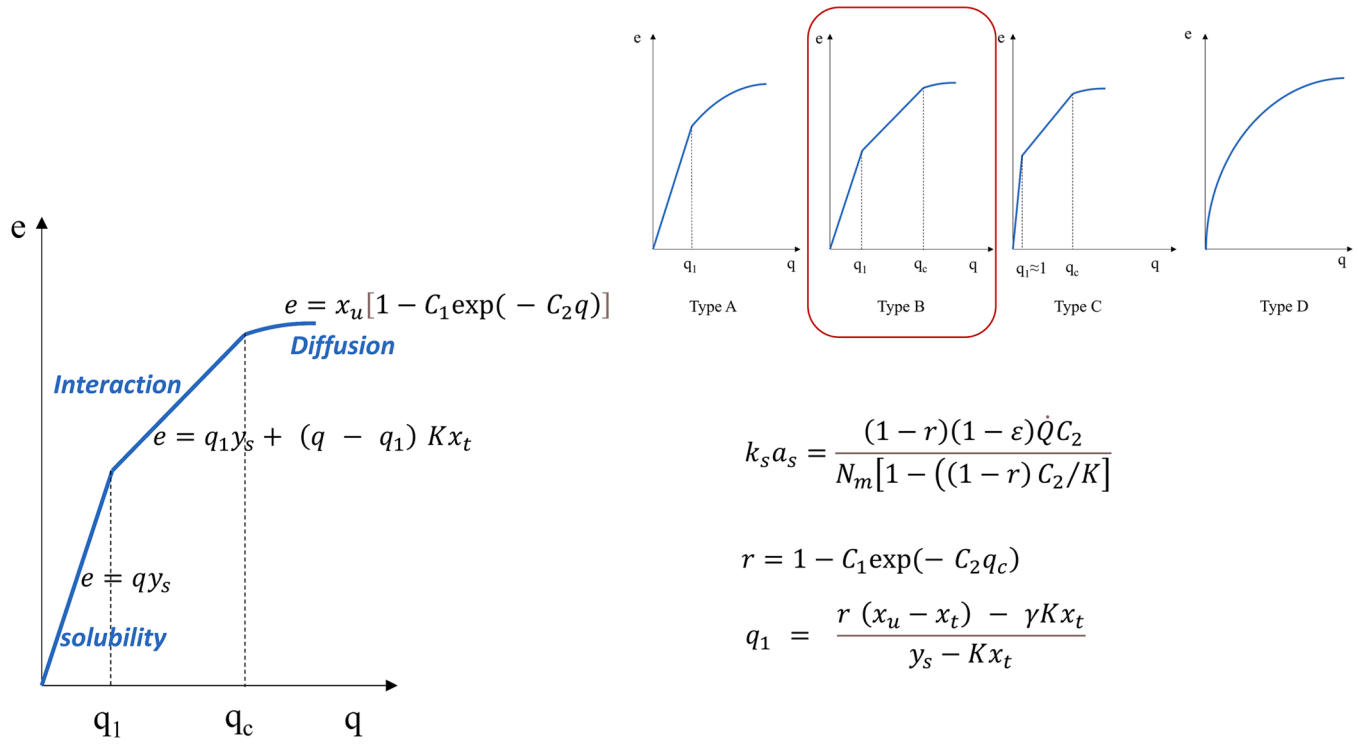

Fig. 2. Type of extraction in Sovová's BIC model.

solute from the biomass. The last part of the extraction curve, described by Eq. (6), is controlled by solute diffusion from intact cells to broken cells.

- First part of the extraction curve

$$e = q y_s \quad \text{for } 0 \le q \le q_1 \tag{3}$$

with *e*, the extraction yield ($kg_{oil}/kg_{insoluble\ biomass}$)

$$q_1 = \frac{r(x_u - x_t) - \gamma K x_t}{y_s - K x_t} \tag{4}$$

$$e = q_1 y_s + (q - q_1) K x_t \quad \text{for } q_1 \le q \le q_c \tag{5}$$

- Second part of the extraction curve

$$e = x_u[1 - C_1 exp(-C_2 q)] \quad \text{for } q > q_c \tag{6}$$

– q_c is the value of q at the crossing point with the estimate for the second part of the extraction curve and

– q_1 is the value of q at the crossing point with the first linear part and the second straight part considering the expression of q_1 in Eq. (4).

The second part of the extraction curve ($q > q_c$) is described by adjusting constant parameters C_1 and C_2. Estimations of parameters $k_s a_s$, the mass transfer coefficient, and *r*, the fraction of the broken cells, can be obtained by considering Eqs. (7)–(12):

$$r = 1 - C_1 exp(-C_2 q_c) \tag{7}$$

$$k_s a_s = \frac{(1-r)(1-\varepsilon)\dot{Q} C_2}{N_m[1-((1-r)C_2/K)]} \quad \text{for } x_t > 0 \tag{8}$$

With:

$$e = \frac{E}{N_m} \tag{9}$$

$$q = \frac{\dot{Q} t}{N_m} \tag{10}$$

$$N_m = (1 - C_u) N \tag{11}$$

$$C_u = \frac{x_u}{1 + x_u} \tag{12}$$

The adjustable parameters "C_1" and "C_2" were calculated by minimising the sum of least squares between the experimental and calculated values of "*e*". The absolute average relative deviation (AARD) between the experimental and calculated yields, was used to evaluate the efficiency of the model. The detailed methodology was given in previous study [2].

3.3. Mass transfer coefficients

To support the discussion about the effect of temperature and flow rate, two transfer parameters were calculated. The first one, the diffusion coefficient of the oil in the supercritical CO_2 (D_{21}) was calculated with the relation of Funazukuri [13] (Eq. (13))

$$D_{21} = \frac{9.671 \times 10^{-14} T}{M^{0.503} \mu^{0.8649}} \tag{13}$$

Where μ is the viscosity of SC-CO_2 and M is the molecular weight of the solute, when dealing with the extraction of C-16 and C-18 lipids, the molecular weight can be represented with the one of triolein 885.4 g/mol [14].

The second calculated parameter was the external (film) mass transfer coefficient k_f that accounts for the external transport of the fluid. The equations reported in the study of del Valle [14] were applied (Eqs. (14)–(17)).

$$Sh = \frac{k_f \times d_p}{D_{21}} \quad (14)$$

With:

$$\mathrm{Sh} = 2 + 1{\cdot}1\mathrm{Re}^{0.6}\mathrm{Sc}^{0.33} \quad (15)$$

$$Sc = \frac{\mu}{D_{21} \times \rho} \quad (16)$$

$$Re = \frac{\rho V D}{(1-\varepsilon) \times \mu} \quad (17)$$

4. Results and discussions

4.1. Repeatability test

A repeatability test (Fig. 3) was performed on two sets of measurements at 400 bar and 333 K and 0.18 kg/h prior to extraction experiments. The average deviation between the two sets of experiments is about 6.1% which is satisfactory.

4.2. Effects of pressure and temperature on the extraction process (Plan A)

The experiments performed in previous study [2] at a CO_2 flow rate of 0.14 kg/h were considered to establish the effect of pressure and temperature on the evolution of y_s and $q_{60\%}$ (Fig. 4).

The polynomial coefficients of Eq. (2) were given in Table 2. The degree of significance of each factor (pressure and temperature) is represented in Table 2 by its p-value in %.

Regarding the evolution of the response y_s, according to the p-values, pressure and temperature appear to be both significant factors which is expected as the evolution of y_s is linked to SC-CO_2 density. On Fig. 4(a), at pressures below 275 bar (in the retrograde solubility zone), the apparent solubility is quite low (lower than 6 $g_{oil}/kg_{solvent}$) and increasing the temperature at a set pressure have no significative influence on the value of y_s: despite a decrease of the apparent solubility with increasing temperature, the values of y_s were at the same order of magnitude. At pressures higher than 300 bar, increasing both pressure and temperature lead to an increase of y_s (from 7 up to 10 $g_{oil}/kg_{solvent}$); at a set temperature, increasing the pressure led to an increase of y_s value. The increase is more pronounced for temperatures higher than 323 K.

Regarding the evolution of the response $q_{60\%}$ (Fig. 4(b)), pressure was reported to be the most significant factor. At pressures below 275 bar (in the retrograde solubility zone), increasing the temperature at a set pressure led to increase the value of $q_{60\%}$ from 250 kg/kg to 850 kg/kg. At pressures ranging from 325 to 360 bar, increasing the temperature at a set pressure didn't lead to a significant change in the value of $q_{60\%}$ which is low in this area (about 150 kg/kg). Finally, increasing the pressure at a set temperature led to a decrease of $q_{60\%}$ value.

Exploring the possibility of applying the SC-CO_2 extraction process at industrial scale, at first approximation, one will consider the operating conditions corresponding to a high apparent solubility of the extracted oil in SC-CO_2 and to the lowest consumption of CO_2 (lowest value of $q_{60\%}$). Fig. 4(a) shows that the highest values of y_s can be reached at pressures ranging from 325 to 400 bar and temperatures ranging from 324 to 333 K. Fig. 4(b) shows that it is advised to work at pressure and temperature ranges located in the blue area delimited by the 150 kg/kg lines. Hence, the intersection of the two delimited areas should be considered as the optimal operating conditions: 325 – 400 bar and 328 – 333 K.

4.3. Effects of temperature and flow rate on the extraction process (Plan B)

Based on previous results, it was chosen to study the effects of flow rate and temperature at a pressure of 400 bar. The effects of flow rate and temperature on the evolution of y_s and $q_{60\%}$ were reported in Fig. 5. The evolution of $q_{60\%}$ is correlated to the evolution of y_s: a high value of y_s leads to a low value of $q_{60\%}$ meaning a low consumption of CO_2 then a low value of y_s leads to a high value of $q_{60\%}$ meaning a high consumption of CO_2. Hence, for the sake of simplicity, only the evolution of y_s will be commented. The polynomial coefficients of Eq. 2 were given in Table 3.

According to the calculated mass transfer coefficients reported in Table 4, increasing the flow rate corresponds to an increase in the mass transfer coefficient. An enhancement of the transfer of oil in SC-CO_2 is thus expected but since contact time is also a significant parameter, it appears that the highest concentration of oil in SC-CO_2 is not observed for the highest flow rate. Indeed, the flow rate has a more complex effect.

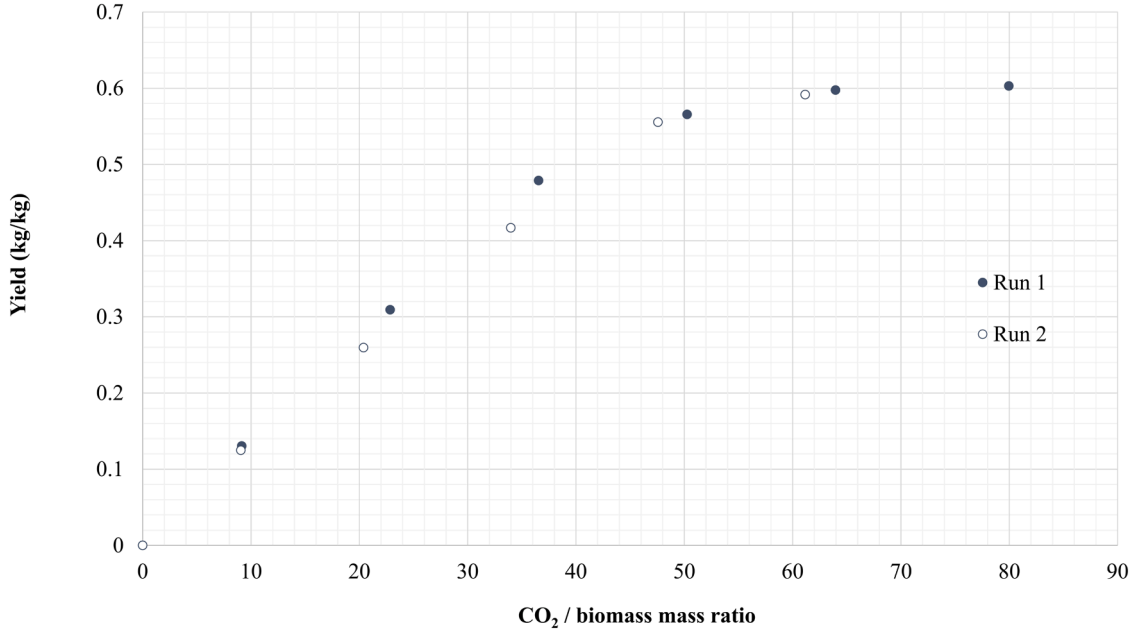

Fig. 3. Reproducibility test perform at 400 bar, 333 K and 0.18 kg/h.

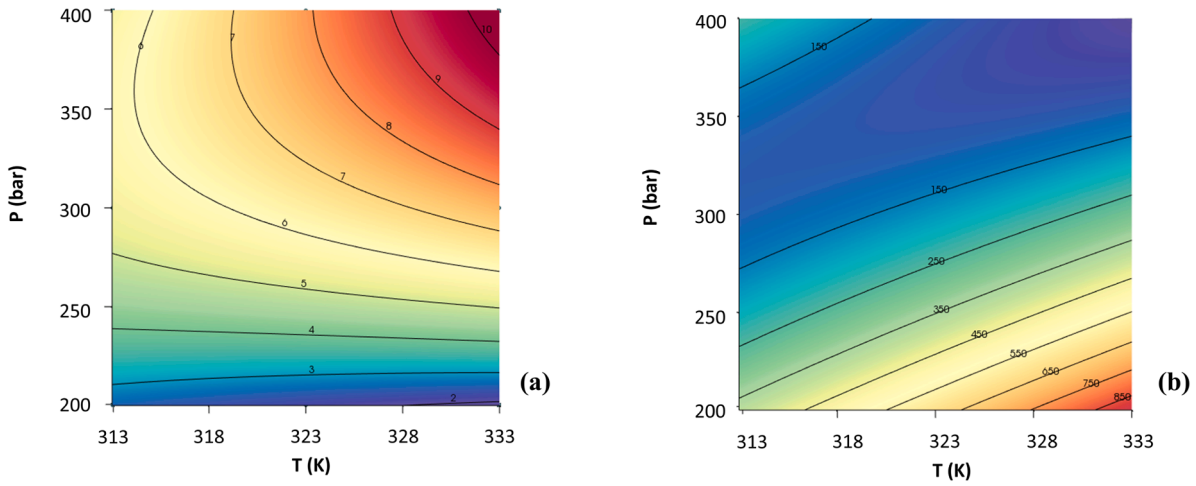

Fig. 4. Surface plot of (a) Argan oil apparent solubility y_s (g_{oil}/kg_{CO2}) in SC-CO_2 and (b) the CO_2/biomass mass ratio ($kg_{CO2}/kg_{biomass}$) for reaching a yield of 60% ($q_{60\%}$) as function of pressure and temperature.

Table 2
Regression coefficients of the polynomial model and analysis of variance for the effects of pressure and temperature on y_s and $q_{60\%}$.

Coefficient	y_s (g_{oil}/kg_{CO2})		$q_{60\%}$ ($kg_{biomass}/kg_{CO2}$)	
	Coefficients values	p-value (%)	Coefficients values	p-value (%)
b_0	6.413	–	174.778	–
b_1	2.873	0.15*	-248.672	1.35*
b_2	1.053	2.50*	87.325	16.32
b_{11}	-1.377	5.12	191.308	10.25
b_{22}	0.0512	91.42	28.108	75.50
b_{12}	1.405	1.99*	-178.75	5.44
R^2	0.98		0.94	

* Significant coefficient.

At a low flow rate, the contact time is longer, leading then to high concentration of oil in SC-CO_2. When the flow rate is increased, the contact time decreases and even if the mass transfer coefficient increases, a lower concentration of oil in SC-CO_2 is observed. For the highest values of flow rate, the contact time is even lower but the effect on the enhancement of convective mass transfer leads to an increase in the concentration of oil in SC-CO_2.

In Fig. 5(a), the value of y_s is higher at a CO_2 flow rate of 0.11 kg/h due to a high SC-CO_2 residence time (t_r) in the extraction autoclave ($8.8 < t_r$ (min) < 9.44), the contact between the solute and SC-CO_2 is then optimal favouring its transfer. At a constant temperature, increasing the SC-CO_2 flow rate up to 0.14 kg/h led to a decrease of y_s value and from 0.14 to 0.18 kg/h a low increase of y_s was observed. It is interesting to notice that the less favourable conditions were found at 0.14 kg/h. At flow rate ranges from 0.16 to 0.18 kg/h the values of y_s

Table 3
Regression coefficients of the polynomial model and analysis of variance for the effects of temperature and flow rate on y_s and $q_{60\%}$.

Coefficient	y_s (g_{oil}/kg_{CO2})		$q_{60\%}$ ($kg_{biomass}/kg_{CO2}$)	
	Coefficient values	p-value (%)	Coefficient values	p-value (%)
b_0	9.135	–	130.426	–
b_1	2.581	3.083 *	-26.579	6.679
b_2	-0.899	27.192	8.917	41.405
b_{11}	-1.788	22.082	9.080	61.697
b_{22}	2.982	8.241	-55.799	4.194 *
b_{12}	-1.195	24.101	5.844	64.762
R^2	0.9		0.88	

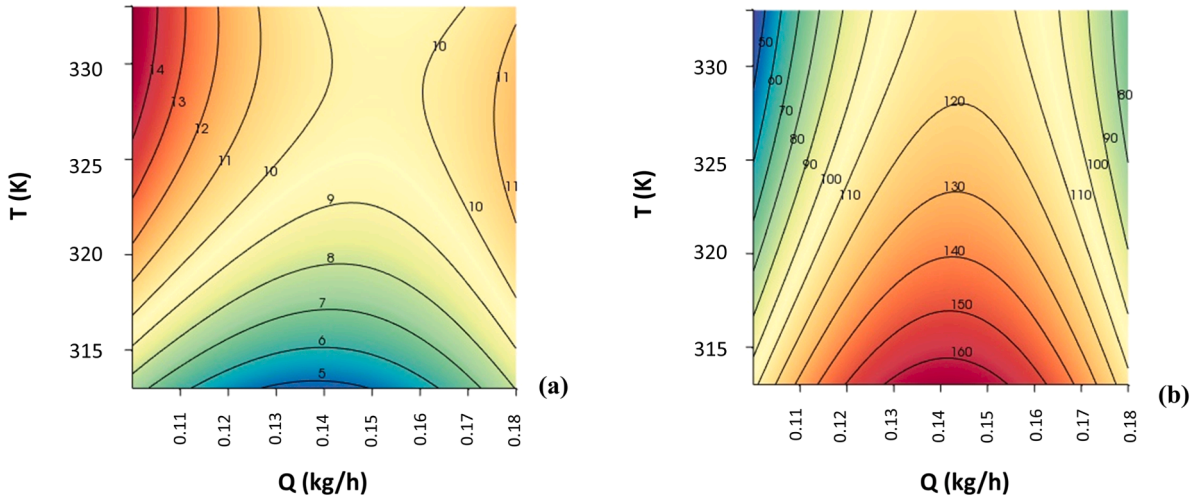

Fig. 5. Surface plot of (a) Argan oil apparent solubility (g_{oil}/kg_{CO2}) in SC-CO_2 and (b) the CO_2/biomass mass ratio ($kg_{CO2}/kg_{biomass}$) for reaching a yield of 60% as function of flow rate and temperature.

Table 4
Mass transfer coefficients and SC-CO_2 residence time at 400 bar.

T (K)	Flow rate (kg/h)	$D_{21} \times 10^9$ (m^2/s)	$k_f \times 10^4$ (s^{-1})	t_r (min)
313	0.11	2.72	1.04	9.44
	0.14		1.26	7.41
	0.18		1.45	5.77
323	0.11	3.04	1.16	9.11
	0.14		1.41	7.16
	0.18		1.62	5.7
333	0.11	3.37	1.29	8.8
	0.14		1.56	6.9
	0.18		1.80	5.37

were close to those found at flow rate range from 0.12 to 0.13 kg/h. Finally, increasing the temperature at a constant flow rate led to an increase of y_s as expected. In this study, it is then obvious that y_s should be considered as the apparent solubility of Argan oil in SC-CO_2. Nevertheless, at a constant temperature, the values of y_s obtained at the three studied flow rates are of the same order of magnitude (Table 5).

The temperature seems to have a more important effect than the flow rate, this point will be developed in the bellow paragraphs. To supplement the observations on Fig. 5, the extraction kinetics were reported in Fig. 6, the BIC model parameters were reported in Table 5.

At a constant temperature (Fig. 6(a-c)), the lowest extraction kinetics were found at a CO_2 flow rate of 0.14 kg/h ($6.9 < t_r$ (min) < 7.41), the fastest extraction kinetic was found at 333 K and 0.11 kg/h. The extraction kinetics were found to be very close at 313 K at 0.11 and 0.18 kg/h and at 333 K at 0.14 and 0.18 kg/h. At a constant flow rate (Fig. 6(d-f)), the extraction kinetics increased with increasing temperature.

The BIC model parameters were reported in Table 5. The parameters were obtained by considering $C_u = 0.64\ kg_{solute}/kg_{solid}$ (asymptotic extraction yield). The values of k_sa_s parameters were found to be close to $1.10^{-5}\ s^{-1}$ except for some experimental conditions. Some values were found to be very high ($10.058\ 10^{-5}\ s^{-1}$) or very low ($0.163\ 10^{-5}\ s^{-1}$). These differences were due to a low number of experimental points in the third part of the extraction curve leading to the determination of parameters C_1 and C_2 values with low accuracy. As the third part is mainly controlled by diffusion, k_sa_s should be independent of flow rate (ksas $\approx 1.10^{-5}\ s^{-1}$).

The shape of the extraction curves (Fig. 6) and the calculated values of y_s bring out that the main difference in the shape of the extraction curves is located in the second part of these curves, the part corresponding to an extraction controlled by solute-matrix interactions. To understand the evolution of the extraction kinetics, it is then necessary to focus on the partition coefficient K. The higher the value of K, the faster the transfer will be in the desorption part of the extraction curve and the faster the extraction kinetics will be. In Table 5, it can be seen that K increases with increasing temperature at a constant flow rate confirming the fact that a high temperature is favourable to the desorption of the oil. The lowest values of K were systematically found at 0.14 kg/h suggesting that, at this flow rate, the extraction is mainly controlled by internal mass transfer resistance. The highest values of K were found at 0.11 and 0.18 kg/h.

At 313 K (Fig. 6(a)) the temperature is quite low for an efficient desorption of the oil, at 0.11 kg/h, the contact time between the extracted oil and the SC-CO_2 is high ($t_r = 9.4$ min), favouriting a saturation of the CO_2-rich phase in oil. This is highlighted by the value of K which is the highest at this condition ($K = 3.387$). Increasing the flow rate up to 0.18 kg/h led to an increase of the extraction kinetic, this surprising result may be due to favourable hydrodynamics conditions due to the higher flow rate.

At 323 K (Fig. 6(b)), the desorption of the oil increases, a competitive effect between mass transfer and driving of the oil may appear. In this case, it seems that the favourable hydrodynamics conditions led to a better extraction kinetics. Nevertheless, at 0.11 kg/h, the high contact time between the solute and SC-CO_2 ($t_r = 9.11$ min) led to a quite good transfer of the solute.

At 333 K (Fig. 6(c)), the temperature is high enough for a good desorption of the oil, the extraction is then mainly controlled by natural desorption. Furthermore, the mass transfer is also good due to a quite high contact time between the oil and SC-CO_2 ($t_r = 8.8$ min at 0.11 kg/h) leading to the highest extraction kinetics. Increasing the flow rate led to an extraction mainly controlled by desorption. Indeed, in Fig. 6(d) and (e) we can see that the evolution of the extraction kinetics at 0.11 and 0.14 kg/h with the temperature is the expected one *i.e* an increase of the extraction kinetics with an increasing temperature. While at 0.18 kg/h (Fig. 6(f)) the evolution of the extraction kinetics according to the temperature clearly suggests that the oil was mainly drive by the flow of SC-CO_2, the contact between the solute and SC-CO_2 is too low ($5.37 < t_r$ (min) < 5.77). Hence, at 333 K Fig. 6(c)), increasing too much the flow rate may lead to higher turbulences which may be unfavourable to the extraction kinetics and to a lower residence time of SC-CO_2 in the extraction autoclave and then a lower contact time between the solute and SC-CO_2. In these experimental conditions it seems that the transfer is mainly controlled by external mass transfer rate.

Considering all these results (Table 4, Figs. 5 and 6), it seems that a residence time of about 9 min at 333 K led to a good contact time

Table 5
BIC model parameters at 400 bar.

T (K)	Q (kg/h)	N (g)	y_s (g_{oil}/kg_{CO2})	C_1	C_2	K_sa_s (s^{-1}) $\times 10^5$	r	K $\times 10^3$	x_t (kg_{oil} / kg insoluble solid)	q_1 ($kg_{solvent}$ / kg_{solid})	q_c ($kg_{solvent}$ / kg_{solid})	γ (kg_{CO2} / $kg_{insoluble\ solid}$)	AARD (%)
313	0.11	6.576	7.239	21.057	0.020	0.775	0.95	3.387	1.707	14.629	94.992	1.328	6.27
	0.14	6.538	5.114	518.879	0.019	10.058	0.91	1.999	1.661	6.938	163.720		3.04
	0.18	6.471	7.183	1.451	0.01	0.848	0.92	3.366	1.701	15.398	95.545		5.10
323	0.11	6.614	11.049	13.287	0.025	1.088	0.94	4.720	1.691	8.328	66.245	1.282	5.80
	0.14	6.503	8.114	130.601	0.021	1.944	0.93	2.591	1.632	5.765	130.815		3.43
	0.18	6.566	13.100	0.113	0.003	0.163	0.93	6.028	1.608	15.431	55.926		8.58
333	0.11	6.648	13.959	4.373	0.026	1.088	0.93	6.840	1.635	15.520	41.649	1.235	10.11
	0.14	6.652	10.600	4.962	0.019	0.906	0.94	4.433	1.597	9.490	76.161		6.20
	0.18	6.589	9.794	1.323	0.012	1.162	0.91	4.538	1.705	9.921	70.490		3.59

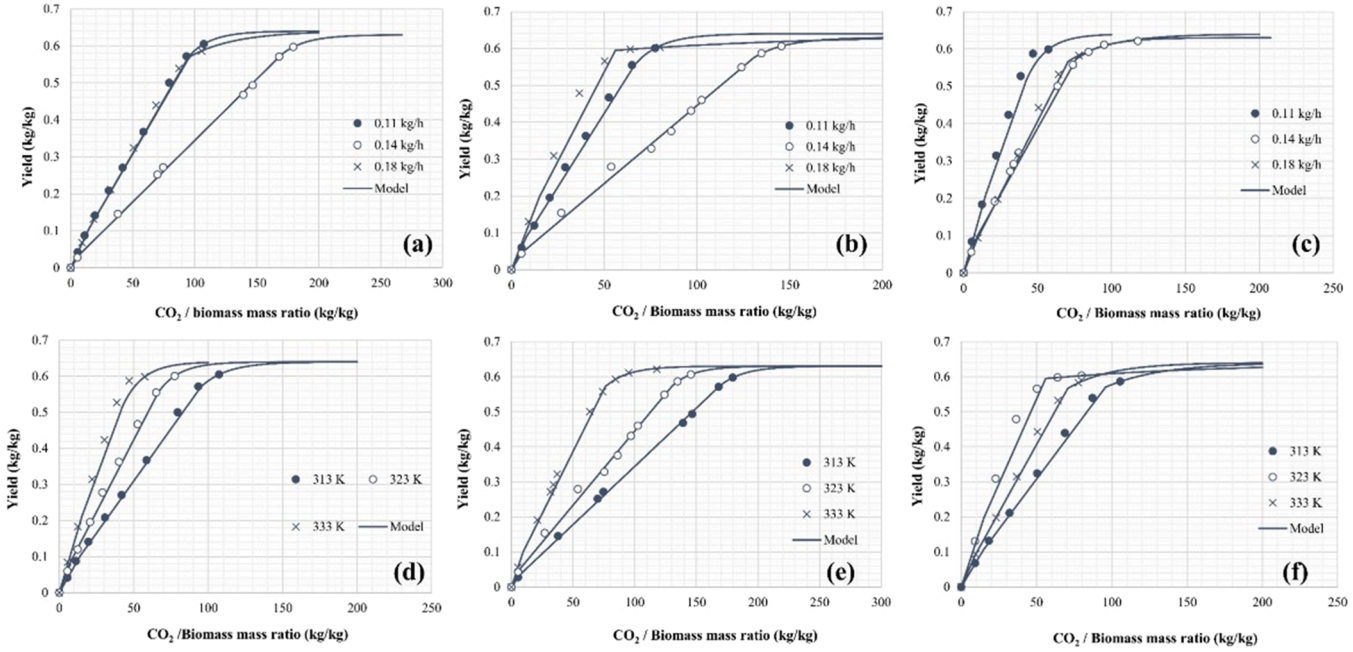

Fig. 6. SC-CO_2 extraction kinetics at 400 bar and (a) 313 K, (b) 323 K, (c) 333 K, at CO_2 flow rate of (d) 0.11 kg/h, (e) 0.14 kg/h and (f) 0.18 kg/h.

between the solute and SC-CO_2 and then a good extraction kinetics.

To confirm this effect of flow rate at 333 K, experiments at 0.14 and 0.27 kg/h were performed at 300 bar. The results were compared to the results published by Taribak et al. [3] at 300 bar, 328 K (closest temperature) at a CO_2 flow rate of 1.2 kg/h. The extraction kinetics and the point obtained by Taribak et al. were reported in Fig. 7. Fig. 7(a) shows that increasing the flow rate was not favourable in terms of extraction kinetics, the transfer is far from equilibrium as the slope of the first part of the extraction curve at 0.27 kg/h is much below the one at 0.14 kg/h. At 1.2 kg/h the extraction kinetic is very low indicating that increasing the flow rate is not favourable.

The residence time at 0.14 and 0.27 kg/h was 6.45 and 3.34 min respectively. The point reported by Taribak et al. was obtained at a residence time of 4.21 min, although the residence time was higher than the one at 0.27 kg/h in this study, the temperature was lower (328 K) leading to less effective desorption explaining the position of the point in Fig. 7(a). Similar tendencies as the one reported at 400 bar were found: the desorption is better at 333 K, a high residence time led to a lower extraction kinetics, and a high flow rate led to mainly drive the solute with SC-CO_2.

In Fig. 7(b) the extraction curves were given as function of the extraction time, at 0.27 kg/h the extraction can be performed faster. Nevertheless, as it was shown in Fig. 7(a), it will require a higher consumption of CO_2. A flow rate of 1.2 kg/h didn't enhance the time of extraction, but it must be kept in mind that the temperature was slightly lower. Hence, the key parameters for an efficient extraction of Argan oil are the temperature (333 K) and the residence time in the empty extraction autoclave (about 9 min).

4.4. *Argan oil analysis*

4.4.1. *Effect of pressure on the FA composition*

Gas chromatography analysis of the fatty acid methyl ester of the oils obtained at 333 K at 300 and 400 bar (Table 6) showed that the oils were mainly composed by palmitic (12 – 13%), stearic (4.5 – 4.9%), oleic (48.5 – 49.25%), and linoleic (31.6 – 32.35%) acids. The relative composition is an agreement with the literature applying conventional and/or SC-CO_2 extraction [3,4,15–20] for Moroccan argan oil.

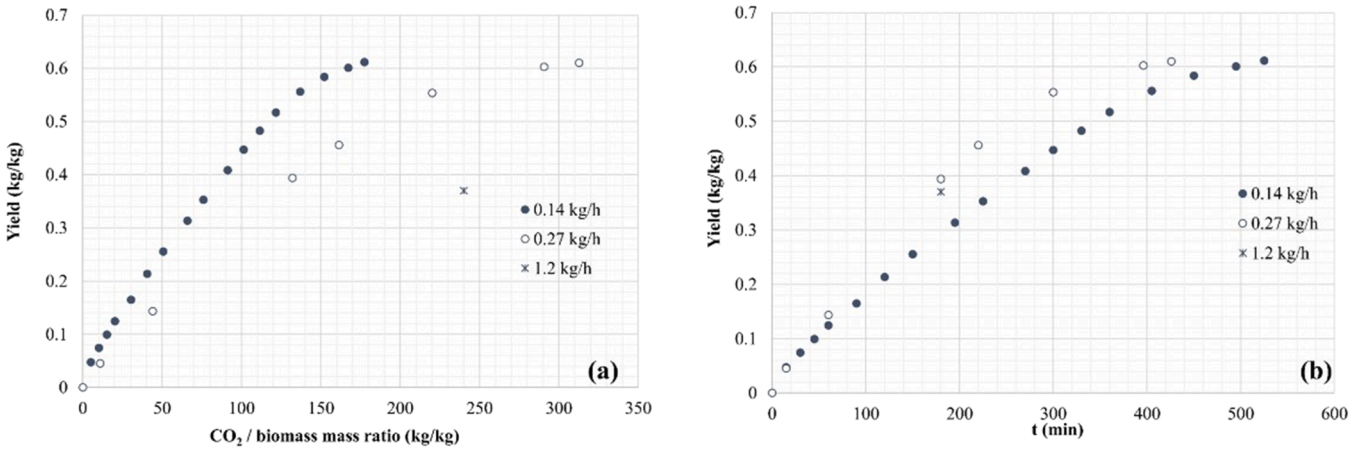

Fig. 7. Extraction kinetics at 300 bar and 333 K. The cross represents the measure obtained by Taribak et al. at 1.2 kg/h, 300 bar and 328 K. (a) Extraction curves as function of CO_2/biomass mass ratio, (b) extraction curves as function of time.

Table 6
FA composition in the oil extracted by SC-CO_2 at 333 K.

	Fatty acid in extracted oil (%)	
Fatty acid	**300 bar**	**400 bar**
16:00	11.97	13.10
16:1ω7	0.11	0.12
17:00	0.07	0.07
18:00	4.89	4.51
18:1ω9	49.25	48.46
18:1ω7	0.23	0.22
18:2ω6	32.25	31.64
20:00	0.32	0.26
20:1ω9	0.34	0.28
Total identified	99.43	98.66

Moreover, the fraction of fatty acid in the extracted oils is similar whatever the pressure.

4.4.2. Effects of extraction period on tocopherol concentration

The aim of this part is to check the possibility of extracting, with SC-CO_2, Argan oil with a high concentration of tocopherols without taking into consideration the fact that the highest reachable yield should be achieved. Indeed, tocopherols are used in cosmetic formulations for their antioxidant properties and guarantee a product's quality.

The oil analysis was performed at 333 K, 300 and 400 bar at 0.14 kg/h at different CO_2/biomass mass ratio corresponding to different positions on the type B extraction curve (solubility, interaction or up to the end). The results are reported in Table 7. Total tocopherol concentration ranged from 640 to 800 mg/kg. The highest tocopherol concentration was obtained at a CO_2/biomass mass ratio ranged from about 10–50 kg/kg corresponding to the interaction part of the extraction curve. The concentration of tocopherols decreased at higher CO_2/biomass mass ratios confirming the hypothesis that tocopherols were mainly extracted at the beginning of the extraction and more precisely in the interaction part of type B extraction curve. In the work previously published by Mouahid et al. [2], it was shown that the concentration of total tocopherols in the oil was the highest at 200 bar and 333 K (1688.6 mg/kg) at a CO_2/biomass mass ratio of 115.5 kg/kg also corresponding to the interaction part of the extraction curve. From these experiments, it appears that to extract a tocopherol rich oil from argan kernels with SC-CO_2, it is advised to work at 200 bar and 333 K until a CO_2/biomass mass ratio of about 115 kg/kg (t_r = 5.6 min). Similar results were reported by Przygoda et al. and Sun et al. [21,22] on the SC-CO_2 extraction of tocopherol from Quinoa seeds and Canola seeds respectively: tocopherols were mainly extracted at 180 – 185 bar (close to 200 bar) [21,22], an increase of pressure didn't enhance the extraction of tocopherols [21,22], the concentration of tocopherol may increase [21] or decrease [22] with increasing time depending on the position on the extraction curve (not given in both studies). Finally, at pressure of about 180 bar increasing the temperature increased the concentration of tocopherols [21,22] which was also reported by Mouahid et al. at 200 bar in previous study on Argan oil [2].

5. Conclusion

Thanks to optimisation study with RSM, the optimal operating conditions leading to the fastest extraction kinetics of Argan oil using SC-CO_2 for cosmetic applications by SC-CO_2 were obtained at 400 bar, 333 K at a CO_2 flow rate of 0.11 kg/h (t_r = 8.8 min). At these operating conditions, the consumption of CO_2 and the extraction time are quite low: about 50 kg/kg (which is in the same order of magnitude as industrial scale), and about 208 min. As the autoclave dimensions (internal length and diameter) may be different from an apparatus to another one, it is more reliable to refer to residence time of SC-CO_2 in the empty extraction autoclave (t_r) for comparison or scale up studies. The Sovová's mathematical model showed that a temperature of 333 K led to a better transfer of the oil in the second part of the extraction curve and to a higher mass transfer due to a high residence time. It was possible to obtain a rich tocopherol oil when the sampling was performed in the interaction part of the extraction curve (CO_2/biomass mass ratio of about 50 kg/kg when pressure ranges from 300 to 400 bar).

The SC-CO_2 extraction process is a very promising clean process to produce Argan oil for cosmetic applications as it is possible to extract all the oil (yield of about 63–64%) from the Argan kernels. Indeed, the extraction yield is higher than conventional extraction method and more or less the same as enzymatic extraction [5]. Compared to conventional and enzymatic extraction, the SC-CO_2 extraction is fastest (few hours), and the extracted oil does not require additional extraction steps like solvent evaporation or settling/centrifugation. Finally, with SC-CO_2 extraction, it is possible to perform sampling at different CO_2/biomass ratios to obtain an oil with a high concentration of tocopherol.

CRediT authorship contribution statement

Adil Mouahid: Conceptualization, Methodology, Software, Validation, Formal analysis, Investigation, Resources, Writing – original draft, Writing – review & editing, Visualization, Supervision, Project administration. **Isabelle Bombarda:** Conceptualization, Methodology, Validation, Formal analysis, Investigation, Writing – original draft, Writing – review & editing. **Magalie Claeys-Bruno:** Conceptualization, Methodology, Validation, Formal analysis, Investigation, Writing – original draft, Writing – review & editing. **Andrea Ciavarella:** Conceptualization, Validation, Formal analysis, Investigation, Writing – original draft. **Sandrine Amat:** Conceptualization, Validation, Formal analysis, Investigation, Writing – original draft, Writing – review & editing. **Emmanuelle Myotte:** Conceptualization, Validation, Formal analysis, Investigation, Writing – original draft, Writing – review & editing. **Jean-Paul Nisteron:** Conceptualization, Validation, Formal analysis, Investigation, Writing – original draft, Writing – review & editing. **Christelle Crampon:** Conceptualization, Methodology, Validation, Formal analysis, Investigation, Writing – original draft, Writing – review & editing. **Elisabeth Badens:** Conceptualization, Methodology, Validation, Formal analysis, Investigation, Writing – original draft, Writing – review & editing, Funding acquisition.

Table 7
Tocopherols concentration at 333 K and 0.14 kg/h at different extraction periods.

P (bar)	α tocopherol (mg/kg $_{extract}$)	γ tocopherol (mg/kg $_{extract}$)	δ tocopherol (mg/kg $_{extract}$)	Total tocopherol (mg/kg$_{extract}$)	Mass of extracted oil (g)	CO_2 / biomass mass ratio (kg/kg)	Position in the extraction curve
300	41.568	538.557	58.036	638.162	0.685	0–15.2	Interaction
	55.388	725.350	41.430	822.168	1.078	15.2–50.7	Interaction
	8.946	183.019	8.673	200.637	2.456	50.7–177	Up to the end
300	41.806	489.473	37.005	568.283	0.248	0–5.6	Solubility
	49.721	724.672	48.081	822.474	0.735	5.6–28.1	Interaction
	15.607	289.681	15.942	321.230	2.845	28.1–196.6	Up to the end
400	42.425	549.898	33.654	625.977	2.141	0–37.2	Interaction
	13.532	217.214	10.225	240.971	1.99	37.2–117.9	Up to the end
400	48.706	588.295	37.596	674.596	0.58	0–11.3	Solubility
	51.149	620.469	38.240	709.857	0.445	11.3–22.6	Interaction

Declaration of Competing Interest

The authors declare that they have no known competing financial interests or personal relationships that could have appeared to influence the work reported in this paper.

Acknowledgements

The authors gratefully acknowledge the support of Giovanna Maria Belogi, Mohammed Mouahid, Moroccan supplier “Chez Brahim, vente de produits naturels Miel et Argan, Av. Mohamed Zerktouni N°41, Essaouira, Morocco” (Agricultural cooperative: Khiorate Biladina) and Thar Process engineers for their help by providing SF100 autoclave dimensions.

Author contribution

The manuscript was written through contributions of all authors. All authors have given approval to the final version of the manuscript. These authors contributed equally.

Appendices.

Dimensions of the extraction autoclave used in this study: internal length = 16 cm, internal diameter = 1.2 cm.

Dimensions of the extraction autoclave used by Taribak et al. [3] according to Thar process: internal length = 14 cm, internal diameter = 3 cm.

References

[1] D. Guillaume, Z. Charrouf, Argan oil and other argan products: Use in dermocosmetology, Eur. J. Lipid Sci. Technol. 113 (2011) 403–408, https://doi.org/10.1002/ejlt.201000417.

[2] A. Mouahid, I. Bombarda, M. Claeys-Bruno, S. Amat, E. Myotte, J.-P. Nisteron, C. Crampon, E. Badens, Supercritical CO_2 extraction of Moroccan argan (Argania spinosa L.) oil: Extraction kinetics and solubility determination, J. CO2 Util. 46 (2021), 101458, https://doi.org/10.1016/j.jcou.2021.101458.

[3] C. Taribak, L. Casas, C. Mantell, Z. Elfadli, R.E. Metni, E.J. Martínez de la Ossa, Quality of cosmetic argan oil extracted by supercritical fluid extraction from *Argania spinosa* L. J. Chem. 2013 (2013) 1–9, https://doi.org/10.1155/2013/408194.

[4] I. Haloui, A.-H. Meniai, Supercritical CO 2 extraction of essential oil from Algerian Argan (Argania spinosa L.) seeds and yield optimization, Int. J. Hydrog. Energy 42 (2017) 12912–12919, https://doi.org/10.1016/j.ijhydene.2016.12.012.

[5] H. Mechqoq, M. El Yaagoubi, S. Momchilova, F. Msanda, N. El Aouad, Comparative study on yields and quality parameters of argan oils extracted by conventional and green extraction techniques, Grain Oil Sci. Technol. (2021), S2590259821000236, https://doi.org/10.1016/j.gaost.2021.08.002.

[6] A. Mouahid, H. Bouanga, C. Crampon, E. Badens, Supercritical CO 2 extraction of oil from Jatropha curcas: An experimental and modelling study, J. Supercrit. Fluids (2017), https://doi.org/10.1016/j.supflu.2017.11.014.

[7] S. Salgın, U. Salgın, Supercritical fluid extraction of walnut kernel oil, Eur. J. Lipid Sci. Technol. 108 (2006) 577–582, https://doi.org/10.1002/ejlt.200600046.

[8] M.G. Bernardo-Gil, M. Casquilho, Modeling the supercritical fluid extraction of hazelnut and walnut oils, AIChE J. 53 (2007) 2980–2985, https://doi.org/10.1002/aic.11299.

[9] M.L. Martínez, M.A. Mattea, D.M. Maestri, Pressing and supercritical carbon dioxide extraction of walnut oil, J. Food Eng. 88 (2008) 399–404, https://doi.org/10.1016/j.jfoodeng.2008.02.026.

[10] H. Sovová, Mathematical model for supercritical fluid extraction of natural products and extraction curve evaluation, J. Supercrit. Fluids 33 (2005) 35–52, https://doi.org/10.1016/j.supflu.2004.03.005.

[11] M. Rahmani, Composition chimique de l’huile d’argane “ vierge ”, Cah. Agric. 14 (2005) 461–465.

[12] G.E.P. Box, The exploration and exploitation of response surfaces: some general considerations and examples, Biometrics 10 (1954) 16, https://doi.org/10.2307/3001663.

[13] T. Funazukuri, C.Y. Kong, S. Kagei, Predictive correlation of binary diffusion and self-diffusion coefficients under supercritical and liquid conditions, J. Supercrit. Fluids 46 (2008) 280–284, https://doi.org/10.1016/j.supflu.2008.03.004.

[14] J.M. del Valle, Extraction of natural compounds using supercritical CO_2: Going from the laboratory to the industrial application, J. Supercrit. Fluids 96 (2015) 180–199, https://doi.org/10.1016/j.supflu.2014.10.001.

[15] M. Hilali, Z. Charrouf, A.E. Aziz Soulhi, L. Hachimi, D. Guillaume, Influence of Origin and Extraction Method on Argan Oil Physico-Chemical Characteristics and Composition, J. Agric. Food Chem. 53 (2005) 2081–2087, https://doi.org/10.1021/jf040290t.

[16] H. Atifi, Z. Bouzoubaâ, S. Gharby, A. Laknifli, R. Mamouni, Fruits maturity effect on the Argan oil amount, quality and chemical composition, 2017. ⟨http://www.jmaterenvironsci.com/Document/vol8/vol8_N2/55-JMES-2710-Atifi.pdf⟩ (accessed 8 June 2017).

[17] R.B. Haloui, A. Zekhnini, A. Hatimi, Effects of extraction methods on chemical composition and oxidative stability of Argan oil, 2015: 8.

[18] M. Kouidri, A. Saadi, A. Noui, F. Medjahed, The Chemical Composition of Argan Oil, 4, 2015: 5.

[19] H. Harhar, S. Gharby, D. Guillaume, Z. Charrouf, Effect of argan kernel storage conditions on argan oil quality, Eur. J. Lipid Sci. Technol. 112 (2010) 915–920, https://doi.org/10.1002/ejlt.200900269.

[20] H. Harhar, S. Gharby, B. Kartah, D. Pioch, D. Guillaume, Z. Charrouf, Effect of harvest date of Argania spinosa fruits on Argan oil quality, Ind. Crops Prod. 56 (2014) 156–159, https://doi.org/10.1016/j.indcrop.2014.01.046.

[21] K. Przygoda, G. Wejnerowska, Extraction of tocopherol-enriched oils from Quinoa seeds by supercritical fluid extraction, Ind. Crops Prod. 63 (2015) 41–47, https://doi.org/10.1016/j.indcrop.2014.09.038.

[22] Q. Sun, J. Shi, M. Scanlon, S.J. Xue, J. Lu, Optimization of supercritical-CO_2 process for extraction of tocopherol-rich oil from canola seeds, LWT 145 (2021), 111435, https://doi.org/10.1016/j.lwt.2021.111435.